*Applied Research on Civil Engineering and Environment (ARCEE)*
*Vol. 05 No.01, February 2024*
*Pages 48-57*

# EXPERIMENTAL STUDY ON STEEL AND POLYPROPYLENE FIBERS MORTAR BOND STRENGTH UNDER UNIAXIAL TENSION

**Herry Suryadi Djayaprabha[1], Wisena Perceka[2*], Angie Oriana[3]**

[1,2,3]*Department of Civil Engineering, Parahyangan Catholic University, Bandung, 40141, Indonesia*

**Corresponding Author: wperceka@unpar.ac.id*

*Received: 2 January 2024; Revised: 22 February 2024; Accepted:28 February 2024*

## ABSTRACT

***The present study aims to investigate the bond behavior between fibers and mortar matrix in fiber-reinforced concrete, which was explored through a uniaxial tension test. The bond behavior was studied for different types of embedded fibers: steel fibers, polypropylene fibers, and hybridizations of steel and polypropylene fibers. The mixture proportion was determined based on the absolute volume method with a water-to-binder ratio (w/b) of 0.29 to achieve high-strength mortar. The high-strength mortar was cast by utilizing an industrial waste by-product of both silica fume and fly ash as a partial cement replacement. The compressive strength and uniaxial tension tests on high-strength mortar were conducted at the ages of 28 and 140 days. The long-term bond-strength behavior was investigated at the age of 140 days. The results showed that the average compressive strengths of hardened mortar on 28 and 140 days were 54.82 MPa and 69.37 MPa, respectively. Whereas, the average fiber-mortar bond strengths with steel, polypropylene, and hybridized fibers were 8.62 MPa, 8.37 MPa, and 7.30 MPa, respectively, at 28 days and 11.22 MPa, 10.21 MPa, and 11.82 MPa, respectively, at 140 days. Compared to the equivalent bond strength of the steel fiber, the polypropylene fiber had an equivalent bond strength of 2.90% and 9.00% lower at the ages of 28 and 140 days. Meanwhile, the equivalent bond strength of hybridized fiber was 15.31% lower than that of steel fiber; however, the long-term behavior of the hybridized fiber showed its performance was about 5,35% higher than that of steel fiber at 140 days.***

**Keywords:** bond strength; high-strength mortar; polypropylene fiber; steel fiber; uniaxial tension test

*DOI: 10.32722/arcee*



## 1. INTRODUCTION

The use of fiber in concrete has increased over time (Ou et al., 2012). The fiber mostly used is steel fiber (Ou et al., 2012; Bhargava et al., 2006; Chao et al., 2009; Liao et al., 2015, 2017; Perceka et al., 2016). With the use of fiber, concrete can reduce its brittleness behavior, especially when concrete experiences tension due to either flexural or direct tension (Liao et al., 2017; Liu et al., 2019). In addition, the presence of steel fibers reduces the post-peak behavior of concrete material, particularly high-strength concrete, under compression since it is well-known that concrete turns more brittle as its compressive strength increases (Bhargava et al., 2006; Liao et al., 2015; Perceka et al., 2016). The reduction of brittleness behavior can occur because the steel fibers can provide bridging action across the microcracks inside the mortar and increase crack opening resistance (Liao et al., 2015; Naaman & Najm, 1991; Perceka et al., 2016; Thomas & Ramaswamy, 2007).

This mechanism can occur due to the presence of the bond strength between steel fibers and the surrounding matrix (Liao et al., 2015; Perceka et al., 2016).

In terms of applying steel fiber to RC structural members, as results showed by Perceka et al. (Perceka et al., 2016) conducted a test on high-strength steel fiber reinforced concrete (SFRC) columns, proving that the early spalling of concrete columns and the early buckling failure of columns with wider transverse reinforcement spacing did not exist. Furthermore, according to the shear tests on SFRC beams reported Perceka et al. (2019), the SFRC beam specimens exhibited non-brittle shear failure as ordinary reinforced concrete (RC) beams showed, i.e., the strength shown by the load-mid. The displacement relationship did not decrease suddenly once the peak strength was reached. In terms of bond strength between steel fibers and the surrounding matrix, it has been reported that the bond strength was affected by fiber geometry, concrete or mortar strength, and fiber material (Liao et al., 2015; Xu et al., 2011).

To the authors' knowledge, previous researchers only performed bond-strength tests by using hooked-end steel fiber. No information about the test on bond strength between fiber and surrounding mortar by using fiber made of materials other than steel, such as polypropylene, has been available. Since polypropylene fibers are commercially available, the potential of the use of polypropylene fibers shall be investigated. Another general consideration when using polypropylene fiber is the corrosion potentially occurring on steel fibers. It is well known that corrosion is a common obstacle when using steel material, although no information has yet been available on the corrosion potential of steel fiber in SFRC material. Regardless of the detailed information on the durability of SFRC material with steel fiber, particularly the effect of corrosion of steel fibers, the potential of the use of polypropylene fiber shall be investigated. The basic information that shall be first investigated is the bond strength between polypropylene fiber and the surrounding mortar since it is well-known that the bond strength has become the main role in improving the behavior of RC members with fibers inside.

Therefore, in this paper, the bond strength between polypropylene fiber and the surrounding mortar was investigated through pullout tests. The specimens used were dog-bone specimens that contained polypropylene fibers. In addition to those specimens, the dog-bone specimens with steel fiber and a combination of steel and polypropylene (hybridized) fibers were prepared as well. By knowing the pullout-slip behavior and bond strength between polypropylene or a combination of steel fiber and polypropylene fibers, more future research regarding the behavior of RC members with fiber other than steel material can be investigated as well.

## 2. METHODS

### 2.1 Materials

In this experimental study, the ternary-blended cementitious materials were composed of Type I ordinary Portland cement (OPC), class F fly ash (FA), and silica fume, which were utilized as binders. Local OPC and FA from Indonesia with specific gravities of 3.03 and 2.13 are being tested (ASTM C188-16, 2016). The commercial densified silica fume had a specific gravity of 2.12 and was tested (ASTM C1240-20, 2020). The fine aggregate had a specific gravity and absorption of 2.49 and 3.09%, which was tested (ASTM C128-15, 2015). The fine aggregate, which conformed to the acceptance range (ASTM C33/C33M-18, 2018), had a fineness modulus (FM) equal to 3.08. The commercial hooked-ended steel and wavy polypropylene fibers were utilized in this study, as shown in Figure 1. The specifications of those fibers are summarized in Table 1. In addition, an acrylic-based superplasticizer (SP) conforming to the requirement (ASTM C494-17, 2017) Type G was used for controlling mortar workability.

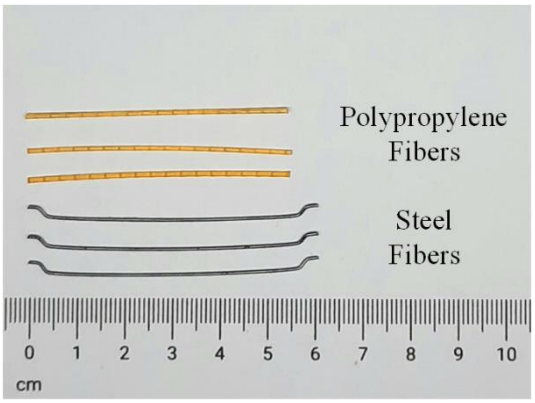


**Figure 1. Physical Appearance of Steel and Polypropylene**

**Table 1. Specification of Steel and Polypropylene Fibers**

| Description | Unit | Steel Fiber (SF) | Polypropylene Fiber (PF) |
|---|---|---|---|
| Length ($L$) | mm | 60 | 55 |
| Diameter ($D$) | mm | 0.75 | 0.91 |
| Aspect Ratio, $L/D$ | - | 80 | 60 |
| Tensile Strength | MPa | 1225 | 560 |
| Modulus of Elasticity | MPa | 200000 | 3900 |
| Type | - | Hooked | Wavy |

## 2.2 Mix Proportions

The mixture proportion mortar was calculated based on the absolute volume method with a water-to-binder ratio (w/b) of 0.29. This number refers to an experimental study conducted by Liao et al. (2015). In addition, Liao et al. (2017) suggested that the total aggregate volume is 0.62 $m^3$, and the FA to fine aggregate ratio is 15%. Moreover, the final amount of cement was replaced with silica fume content by mass, in the amount of 10% of the binder mass. In addition, SP based on a modified acrylic polymer was used at a fixed amount of 1.5% of the total powder mass to establish the expected fresh mortar properties. The final mix proportion of the mortar after performing the necessary trial-and-error procedure and modification is listed in Table 2.

**Table 2. Mixture Proportion of Mortar**

| Material | Quantities ($kg/m^3$) |
|---|---|
| Cement | 422.9 |
| Fly Ash | 231.4 |
| Silica Fume | 81.8 |
| Water | 213.5 |
| Fine Aggregate | 1542.6 |
| Superplasticizer | 11.0 |

## 2.3 Specimen Preparation and Testing Methods

The dog-bone specimens with detailed geometry and dimensions, as shown in Figure 2(a), were used to determine the bond strength between the fibers and mortar matrix. A single dog-bone specimen with ten embedded fibers in the middle section was separated into two sides. There were three configurations of fiber,

as demonstrated in Figure 2(b); they were full steel fibers (SF), full polypropylene fibers (PF), and hybridizations of steel and polypropylene fibers (HF). Three dog-bone specimens were prepared for each configuration. An acrylic mold, as shown in Figure 3(a), was used for casting a dog bone specimen. As shown in Figure 3(b), a foam block with clinging film was equipped to mount the fibers in the middle part of the mold. The casting process of the dog-bone specimen was completed within two days. On the first day, the fresh mortar was poured into half of the dog bone specimen until the mounted fibers were completely cast, as demonstrated in Figure 3(c). On the following day, the foam block was carefully removed from the middle part, and the clinging film still stuck in the middle part, as shown in Figure 3(d), then filled the mold with fresh mortar until the other part was completely cast, as demonstrated in Figure 3(e). The bond strength tests were conducted in an electro-hydraulic servo universal testing machine (UTM) with a capacity of 500 kN (brand Hung-Ta model HT9501, serial number 1162) at a displacement rate of 0.6 mm/min. The UTM was equipped with a pair of steel testing grips, as demonstrated in Figure 4, for mounting the dog bone specimen. In addition, a digital single-lens reflex camera was used to digitally capture the pullout slip of the dog-bone specimen. In this study, the mortar-fiber bond strength tests were investigated at 28 and 140 days. At least duplicate 50-mm cubic specimens were made from each side of the casting to determine the compressive strength of mortar specimens in accordance with ASTM C109/C109M (ASTM C109/C109M, 2021). The tests were performed at 28 and 140 days by utilizing a semi-automatic compression machine with a capacity of 2000 kN (ELE model ADR2000) at a constant rate of 0.9 kN/s. According to ASTM C109/C109M (ASTM C109/C109M, 2021), the compressive strength of mortar ($fm$) is calculated by dividing the load at failure (P) with the cross-sectional area of the mortar cube (A) as described in Equation (1).

$$fm = \frac{\mathrm{P}}{\mathrm{A}} \tag{1}$$

According to Liao et al. (Liao et al., 2015), the equivalent bond strength ($\tau_{\mathrm{eq}}$) of each fiber configuration can be calculated by using Equation (2). It is shown that $\tau_{\mathrm{eq}}$ is the function of fiber pullout energy ($E_{\mathrm{po}}$) that is expressed by the area under the pullout load-slip curve, fiber diameter ($d_{\mathrm{f}}$), and the embedded length of the fiber ($L^2_{\mathrm{emb}}$).

$$\tau_{\mathrm{eq}} = \frac{2E_{\mathrm{po}}}{\pi \cdot d_{\mathrm{f}} \cdot L^2_{\mathrm{emb}}} \tag{2}$$

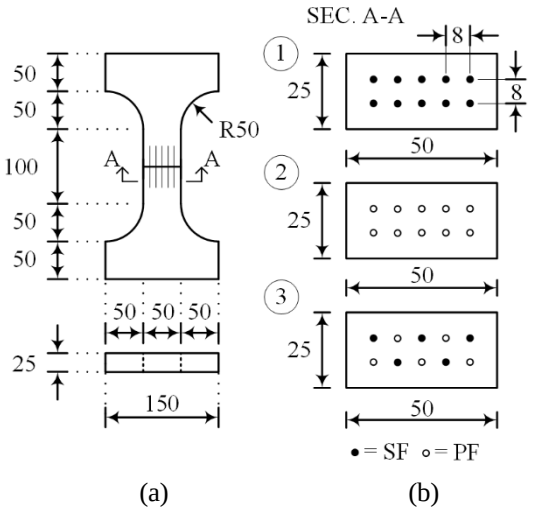


**Figure 2. (a) The Geometry and Dimensions of Specimen; (b) Fiber Configurations**


(a) (b) (c) (d) (e)

**Figure 3. Example of Casting Procedures of Dog-Bone Specimen with Steel Fibers**

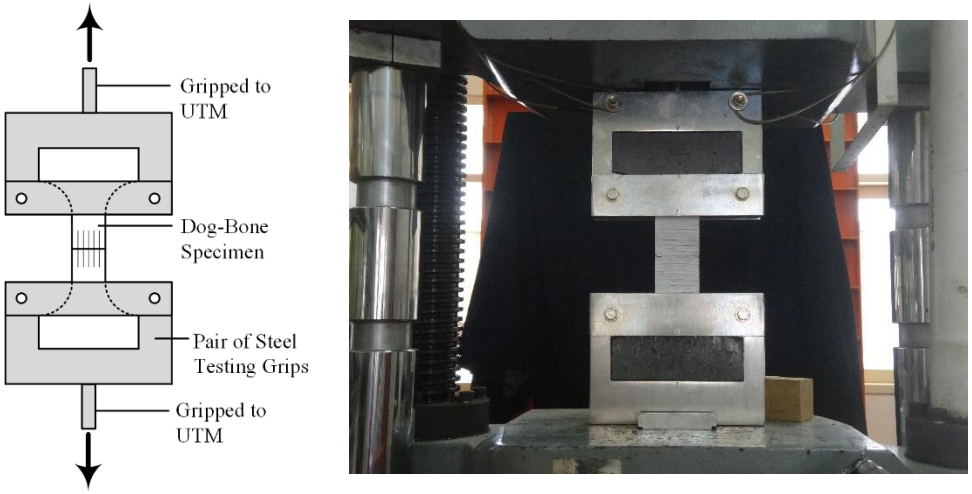


(a) (b)

**Figure 4. (a) Schematic Test Setup; (b) Test Setup Documentation**

## 3. RESULTS AND DISCUSSION

### 3.1 Compressive Strength

As reported by Liao et al. (2017), the equivalent bond strength of fiber increased as the compressive strength of the mortar matrix increased. Therefore, the bond strength of fibers in the mortar is affected by the matrix compressive strength. In this study, the compressive strength tests for each variation were tested at the age of 28 and 140 days. As summarized in Table 3, the average 28-day compressive strength of the mortar matrix ($fm$) was 55.08 MPa with a standard deviation ($\sigma$) and coefficient of variation (CV) of 2.78 MPa and 5.05%, respectively. Furthermore, it was observed that the 140-day compressive strength was 27.60% higher than the 28-day compressive strength. The incorporation of the silica fume into the mortar matrix induced higher long-term compressive strength due to the pozzolanic reaction that consumes a huge amount of portlandite and forms more C-S-H gel (Tavares et al., 2020; Fu et al., 2021).

**Table 3. Summary of the Compressive Strength**

| Age (days) | $fm$ (MPa) | $\sigma$ (MPa) | CV (%) |
|---|---|---|---|
| 28 | 55.08 | 2.78 | 5.05 |
| 140 | 70.28 | 4.73 | 6.73 |

## 3.2 Equivalent Bond Strength

The equivalent bond strength average ($\bar{\tau}_{eq}$) was calculated by averaging the results obtained from three tests, as summarized in Table 4. The symbols SF, PH, and HF, respectively, stood for steel fibers, polypropylene fibers, and hybrid fibers. The equivalent bond strengths of those three different configurations were investigated at days 28 and 140. Figure 5 demonstrates the pullout load-slip curves of all specimens. In each test, the $E_{po}$ was determined by calculating the area under the pullout load-slip curve, and the $\tau_{eq}$ was determined by using Equation (2). As presented in Table 4, the SF exhibited the highest bond strength, with an average value of 7.30 MPa at 28 days and 9.70 MPa at 140 days. In the meantime, the average bond strengths of PF specimens at 28 days and 140 days, respectively, were 6.74 MPa and 8.57 MPa. In addition, the 28-day and 140-day bond strengths of HF specimens were 7.13 MPa and 9.15 MPa, respectively.

Compared to the average bond strength of the SF specimen, it can be seen that the 28-day average bond strength of the PF and that of the HF specimens, respectively, were 7.67% and 2.33% lower. In addition to the comparison for days 28, the average bond strength of PF and that of HF specimens at 140 days decreased by 11.65% and 5.67 %, respectively, when compared to the average bond strength of SF at days 140. It can be noted that the SF specimen exhibited the highest bond strength due to the mechanical anchorage of the hooked end at each edge of the fiber (Abdallah et al., 2018). Unlike the hooked-end steel fiber, polypropylene, in general, relies only on the friction force between the fiber and the surrounding mortar. On the other hand, the HF specimen demonstrated a higher bond strength compared to the PF specimen; however, the bond strength of the HF specimen was lower than that of the SF specimen. In the HF specimen, the friction steel fiber-surrounding mortar and the mechanical anchorage action due to hooked-end steel fiber still exist. Therefore, the HF specimen could exhibit higher strength compared to the PF specimen. In the meantime, the reduction in the number of steel fibers in the HF specimen led to a reduction in bond strength when compared to the SF specimen. Moreover, at the age of day 140, the average bond strengths of SF, PF, and HF increased by 32.88%, 27.15%, and 28.33%, respectively, compared to the strengths at day 28. Therefore, the improvement of mortar strength led to the improvement of bond strength generally (Ding et al., 2021).

**Table 4 Equivalent bond strength results**

| Mixture Code† | No | 28 days | | 140 days | |
|---|---|---|---|---|---|
| | | $\tau_{eq}$ (MPa) | $\bar{\tau}_{eq}$ (MPa) | $\tau_{eq}$ (MPa) | $\bar{\tau}_{eq}$ (MPa) |
| SF0.29 | (1) | 8.17 | 7.30 | 9.76 | 9.70 |
| | (2) | 7.29 | | 9.64 | |
| | (3) | 6.45 | | 9.69 | |
| PF0.29 | (1) | 6.95 | 6.74 | 9.46 | 8.57 |
| | (2) | 7.13 | | 7.98 | |
| | (3) | 6.14 | | 8.27 | |
| HF0.29 | (1) | 6.69 | 7.13 | 8.88 | 9.15 |
| | (2) | 8.52 | | 8.68 | |
| | (3) | 6.19 | | 9.89 | |

†Note: PF=Polypropylene Fiber, SF=Steel Fiber, HF=Hybrid Fiber, and the numbers denote the water-to-binder ratio

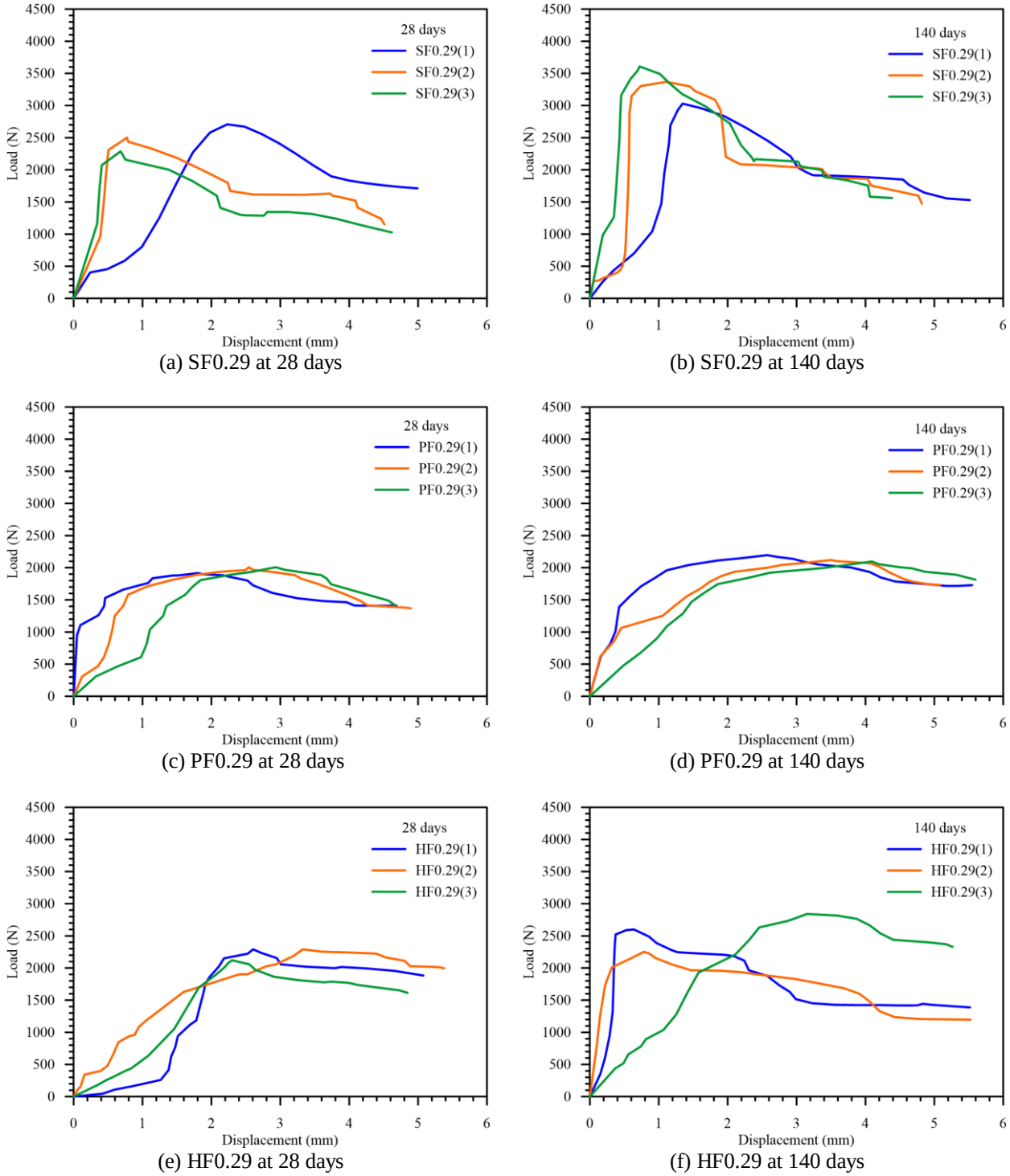


(a) SF0.29 at 28 days (b) SF0.29 at 140 days

(c) PF0.29 at 28 days (d) PF0.29 at 140 days

(e) HF0.29 at 28 days (f) HF0.29 at 140 days

**Figure 5. Equivalent bond strength of SF, PF, and HF**

## 3.2 Failure Modes

Figure 6 presented the typical failure modes of SF, PF, and HF specimens after pullout tests at days 28 and 140. The failure modes of all SF specimens with SF were bond-slip, as seen in Figures 6(a) and (b), regardless of the days of the test performed. In addition, the PF specimens tested on day 28 failed due to the slip of fiber in the mortar. In contrast, after 140 days, it was found that two polypropylene fibers of the PF specimen got broken, as shown in Figure 6(d). This phenomenon indicated the bond strength might be higher than the tensile

strength of polypropylene fiber in the long-term period since the mortar strength could still develop after days 28 (Ding et al., 2021). A broken fiber was only found in the PF specimen, while no broken fiber occurred in the SF and HF specimens, as seen in Figures 6(e) and (f). It must be noticed that the tensile strength of steel fiber is much greater than that of polypropylene fiber. Therefore, by keeping steel fiber inside the HF specimen, the bond strength between the single fiber and surrounding mortar could be lower and could be broken before the broken fiber occurred. The final appearance of the steel fiber in this study also confirmed the mechanism of the steel fiber pullout test reported by Liao et al. (2015).

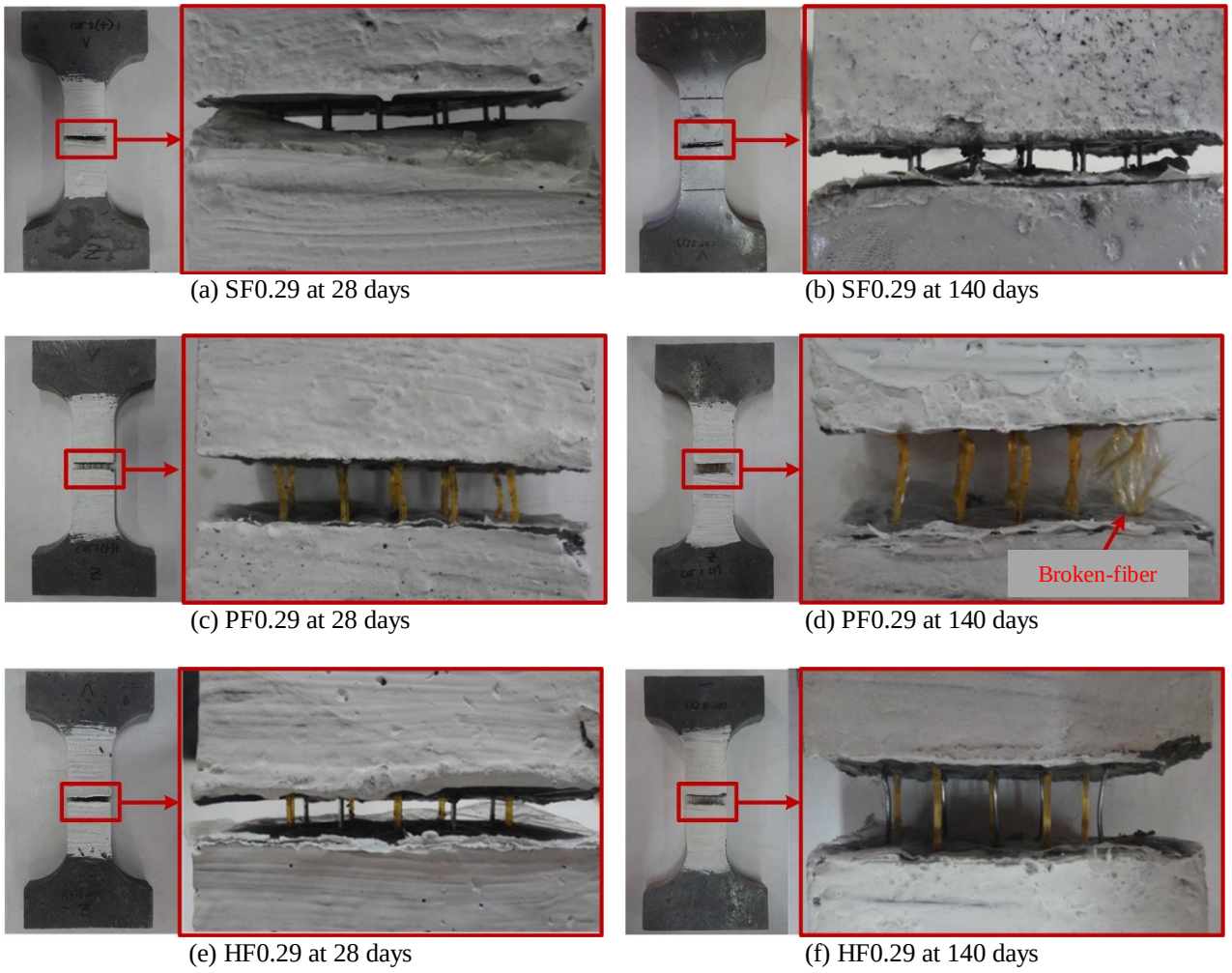


(a) SF0.29 at 28 days (b) SF0.29 at 140 days

(c) PF0.29 at 28 days (d) PF0.29 at 140 days

(e) HF0.29 at 28 days (f) HF0.29 at 140 days

**Figure 6. Typical failure mode of dog-bone specimens after pullout test**

## 4. CONCLUSIONS

The bond strengths of steel fibers, polypropylene fibers, and hybridizations of steel and polypropylene fibers on cement-based high-strength mortar matrix incorporated with silica fume and fly ash were successfully investigated by involving different fiber configurations in the dog-bone specimens and performing tests at different times in order to capture the short-and long-term effects. The SF specimens exhibited the highest equivalent bond strength among the three type configurations since the equivalent bond strength of the SF specimen is affected by both the steel fiber surface-surrounding mortar friction force and the mechanical anchorage action due to hooked-end steel fiber. In contrast, the equivalent bond strength of the fiber and surrounding mortar of the PF specimen only relied on the fiber surface-surrounding mortar friction force. Furthermore, in the HF specimen, due to the presence of steel and polypropylene fibers, the equivalent bond strength was affected by the fiber surface-surrounding mortar friction force that appeared from steel and polypropylene fibers and the mechanical anchorage action due to hooked-end steel fiber. In terms of failure

mode, the failure mode of SF and HF specimens was a bond-slip failure, while the failure mode of PF specimens was the rupture of fibers. In addition, according to the failure modes shown by SF, PF, and HF specimens, it can be noticed that the presence of steel fibers affected the failure mode and tended to turn the rupture of fiber into bond-slip failure. This study presents the long-term effects as well. It is known that the equivalent bond strength at day 140 was greater than that at day 28, regardless of the fiber configuration. Since polypropylene fiber is commercially available, further study in terms of the use of polypropylene fiber in FRC structural members may be necessary. However, based on the fiber pullout behavior, the value of equivalent bond strength, and referring to previous studies of FRC structural members, the steel fibers could exhibit better performance in FRC structural members compared to the polypropylene fibers.

## ACKNOWLEDGEMENT

The authors would like to express their gratitude for the financial support provided by Lembaga Penelitian dan Pengabdian kepada Masyarakat (LPPM) Universitas Katolik Parahyangan through grant No. III/LPPM/2020-01/29-P and PT. Mapei Indonesia Construction Product through memorandum of agreement No. III/AU/FT/2019-11/1665-E, which facilitated the procurement of polypropylene fibers and concrete admixtures for this experimental study. The results, opinions, and discussions presented here are those of the authors and do not represent the sponsors.

## REFERENCES

Abdallah, S., Fan, M., & Rees, D. W. A. (2018). Bonding Mechanisms and Strength of Steel Fiber–Reinforced Cementitious Composites: Overview. *Journal of Materials in Civil Engineering*, *30*(3). https://doi.org/10.1061/(ASCE)MT.1943-5533.0002154

ASTM C33/C33M-18. (2018). *Standard Specification for Concrete Aggregates*. West Conshohocken, ASTM International.

ASTM C109/C109M. (2021). *Standard Test Method for Compressive Strength of Hydraulic Cement Mortars (Using 2-in. or [50-mm] Cube Specimens)*. West Conshohocken, ASTM International.

ASTM C128-15. (2015). *Standard Test Method for Relative Density (Specific Gravity) and Absorption of Fine Aggregate*. West Conshohocken, ASTM International.

ASTM C188-16. (2016). *Standard Test Method for Density of Hydraulic Cement.* West Conshohocken, ASTM International.

ASTM C494-17. (2017). *Standard Specification for Chemical Admixtures for Concrete*. West Conshohocken, ASTM International.

ASTM C1240-20. (2020). *Standard Specification for Silica Fume Used in Cementitious Mixtures*. West Conshohocken, ASTM International.

Bhargava, P., Sharma, U. K., & Kaushik, Surendra. K. (2006). Compressive Stress-Strain Behavior of Small Scale Steel Fibre Reinforced High Strength Concrete Cylinders. *Journal of Advanced Concrete Technology*, *4*(1), 109–121. https://doi.org/10.3151/jact.4.109

Chao, S.-H., Naaman, A. E., & Parra-Montesinos, G. J. (2009). Bond Behavior of Reinforcing Bars in Tensile Strain-Hardening Fiber-Reinforced Cement Composites. *ACI Structural Journal*, *106*(06). https://doi.org/10.14359/51663191

Ding, X., Zhao, M., Li, C., Li, J., & Zhao, X. (2021). A multi-index synthetical evaluation of pullout behaviors of hooked-end steel fiber embedded in mortars. *Construction and Building Materials*, *276*, 122219. https://doi.org/10.1016/j.conbuildmat.2020.122219

Fu, C., Guo, R., Lin, Z., Xia, H., Yang, Y., & Ma, Q. (2021). Effect of nano silica and silica fume on the mechanical properties and microstructure of lightweight engineered cementitious composites. *Construction and Building Materials*, *298*, 123788. https://doi.org/10.1016/j.conbuildmat.2021.123788

Liao, W.-C., Perceka, W., & Liu, E.-J. (2015). Compressive Stress-Strain Relationship of High Strength Steel Fiber Reinforced Concrete. *Journal of Advanced Concrete Technology*, *13*(8), 379–392. https://doi.org/10.3151/jact.13.379

Liao, W.-C., Perceka, W., & Yu, L.-C. (2017). Systematic Mix Procedures for Highly Flowable-Strain Hardening Fiber Reinforced Concrete (HF-SHFRC) by Using Tensile Strain Hardening Responses as Performance Criteria. *Science of Advanced Materials*, *9*(7), 1157–1168. https://doi.org/10.1166/sam.2017.3097

Liu, C., Zhang, Y., Yao, Y., & Huang, Y. (2019). Calculation method for flexural capacity of high strain-hardening ultra-high performance concrete T-beams. *Structural Concrete*, *20*(1), 405–419. https://doi.org/10.1002/suco.201800151

Naaman, A. E., & Najm, H. (1991). Bond-Slip Mechanisms of Steel Fibers in Concrete. *ACI Materials Journal*, *88*(2). https://doi.org/10.14359/1896

Ou, Y.-C., Tsai, M.-S., Liu, K.-Y., & Chang, K.-C. (2012). Compressive Behavior of Steel-Fiber-Reinforced Concrete with a High Reinforcing Index. *Journal of Materials in Civil Engineering*, *24*(2), 207–215. https://doi.org/10.1061/(ASCE)MT.1943-5533.0000372

Perceka, W., Liao, W.-C., & Wang, Y. (2016). High Strength Concrete Columns under Axial Compression Load: Hybrid Confinement Efficiency of High Strength Transverse Reinforcement and Steel Fibers. *Materials*, *9*(4), 264. https://doi.org/10.3390/ma9040264

Perceka, W., Liao, W.-C., & Wu, Y.-F. (2019). Shear Strength Prediction Equations and Experimental Study of High Strength Steel Fiber-Reinforced Concrete Beams with Different Shear Span-to-Depth Ratios. *Applied Sciences*, *9*(22), 4790. https://doi.org/10.3390/app9224790

Tavares, L. R. C., Junior, J. F. T., Costa, L. M., da Silva Bezerra, A. C., Cetlin, P. R., & Aguilar, M. T. P. (2020). Influence of quartz powder and silica fume on the performance of Portland cement. *Scientific Reports*, *10*(1), 21461. https://doi.org/10.1038/s41598-020-78567-w

Thomas, J., & Ramaswamy, A. (2007). Mechanical Properties of Steel Fiber-Reinforced Concrete. *Journal of Materials in Civil Engineering*, *19*(5), 385–392. https://doi.org/10.1061/(ASCE)0899-1561(2007)19:5(385)

Xu, B. W., Ju, J. W., & Shi, H. S. (2011). Progressive Micromechanical Modeling for Pullout Energy of Hooked-end Steel Fiber in Cement-based Composites. *International Journal of Damage Mechanics*, *20*(6), 922–938. https://doi.org/10.1177/1056789510385260